Supplementary Information

Facile Fabrication of Hierarchical Rh_2Ir Alloy Nanodendrites with Excellent HER Performance in a Broad pH Range

Qicheng Liu ‡ [a], Chuang Fan ‡ [a], Xinyi Zhou [a], Jiaqi Liu [a], Shuang Jiang [a], Siyuan Wang [a], Xiaojun Wang *[b], Yawen Tang *[a]

[a] Jiangsu Key Laboratory of New Power Batteries, Jiangsu Collaborative Innovation Centre of Biomedical Functional Materials, School of Chemistry and Materials Science, Nanjing Normal University, Nanjing 210023, China. tangyawen@njnu.edu.cn (Y. Tang)

[b] School of Life Sciences, Nanjing Normal University, Nanjing, 210023, China. wangxiaojun0910@njnu.edu.cn (X. Wang)

‡ Q. Liu and C. Fan contributed equally to this work.

Experimental Section

Chemicals and Materials

Polyallylamine hydrochloride (PAH) (weight-average molecular weight 5,000) was supplied by Nitto Boseki Co., Ltd. (Tokyo, Japan). Iridium chloride and rhodium chloride were purchased from DB Biotechnology Co., Ltd. (Shanghai, China). Ethylene glycol, absolute ethyl alcohol (EG) and formic acid (88%) were purchased from Sinopharm Chemical Reagent Co., Ltd (Shanghai, China). Commercial Pt/C, Pt black and Pd black were purchased from Johnson Matthey Corporation. All the reagents were not further purified. All the reactions will take place in serum flasks that can withstand high temperatures.

Synthesis of the Rh_2Ir NDs

In a typically synthesis, ethylene glycol solution of iridium chloride (0.3 mL, 0.05 M), ethylene glycol solution of rhodium chloride (0.3 mL, 0.05 M) and formic acid (1 mL, wt = 88%) were added to a continuously stirred solution, which has been thoroughly and evenly mixed with 0.5 mL of PAH (wt 40%) in 15 mL ethylene glycol, respectively. The serum flask was kept in a methyl silicone oil bath for preheating 0.5 h at 120 ℃. The temperature is then raised to 200 ℃, and the temperature is heated at a rate of 4 ℃/min. After the temperature stabilizes, it reacts for 0.5 h. After the reaction, the black nano chrysanthemums (NDs) were separated by centrifugation at 11,000 rpm for 20 min, washed several times with DI water and absolute ethyl alcohol. Finally, dried at the vacuum freeze dryer at 70 ℃ for 24 h in a clean beaker.

Synthesis of the RhIr sample

The PAH (wt 40%) was diluted into a dilute solution in a ratio of 0.5 mL to 5 mL deionized (DI) water. When fully mixed, 1mL of the prepared PAH solution was dispersed in 15mL of ethylene glycol solution under continuous string. After the homogeneous dispersion, ethylene glycol solution of iridium chloride (0.3 mL, 0.05 M), ethylene glycol solution of rhodium chloride (0.3 mL, 0.05 M) and formic acid (2 mL, wt = 88%) were added to the solution, respectively. The serum flask was kept in a methyl silicone oil bath for preheating 0.5 h at 120 ℃. The temperature is then raised to 200 ℃, and the temperature is heated at a rate of 4 ℃/min. After the temperature stabilizes, it reacts for 4 h. After the reaction, the black products were separated by centrifugation at 18,000 rpm for 10 min, washed several times with DI water, and dried at the vacuum freeze dryer at -70 ℃ for 24 h in a clean beaker.

Synthesis of the Rh sample

The ethylene glycol solution of rhodium chloride (0.3 mL, 0.05 M) and formic acid (1 mL, wt = 88%) were added to a continuously stirred solution, which has been thoroughly and evenly mixed with 0.5 mL of PAH (wt 40%) in 15 mL ethylene glycol, respectively. The serum flask was kept in a methyl silicone oil bath for preheating 0.5 h at 120

℃. The temperature is then raised to 200 ℃, and the temperature is heated at a rate of 4 ℃/min. After the temperature stabilizes, it reacts for 1 h. After the reaction, the black products were separated by centrifugation at 11,000 rpm for 20 min, washed several times with DI water and absolute ethyl alcohol. Finally, dried at the vacuum freeze dryer at -70 ℃ for 24 h in a clean beaker.

Physicochemical Characterization

The morphology and microstructure of the Rh_2Ir NDs by TEM and HRTEM, which were acquired on a JEOL JEM-2100F transmission electron microscopy manipulated with an accelerating voltage of 200 kV. The HAADF-STEM images were acquired on JEOL JEM-ARM 200F. EDS measurements were conducted on an Oxford Instruments ULTIM MAX 170. The concentrations of metals were then measured with a Thermo Scientific PlasmaQuad 3inductively-coupled plasma mass spectrometry (ICP-MS) and EDS. XPS measurements were conducted on a Thermo VG Scientific ESCALAB 250 spectrometer with an Al Kα radiator. The binding energy was calibrated by means of the C 1s peak energy of 284.6 eV. XRD analyses were performed on a Model D/max-rC X-ray diffractometer employing Kα radiation (λ = 0.15406 nm). BET measurements were required on MicrotracBEL BELSORP-max with adsorptive of N_2. The apparatus temperature and adsorption temperature are 0 ℃ and 77 K, respectively.

Electrochemical Measurements

Electrochemical measurements were performed on a CHI 760E CH analyser (Shanghai, Chenhua Co.) with a conventional three-electrode system. All potentials reported in this work were transformed to the reversible hydrogen electrode (RHE), and the conversion formula was as follows: $E_{RHE} = E_{SCE} + 0.0592\ pH + 0.242$. The 2 mg catalyst was dissolved in 1 mL of DI water and the homogenous catalyst suspension was prepared by at least 30 min ultrasonic dispersion uniformity. Then 5 μL of catalyst solution could added to the prepared bright and clean surface of the electrode. Dry at room temperature and add again. After 4 repetitions, 2.5 μL of Nafion solution (5 wt%) was layered on the surface of the modified electrode and allowed to dry. After dying again, the working electrode was obtained. The stable cyclic voltammetry (CV) measurements, to probe the current capacity, were conducted in N_2-protected 1 M $HClO_4$ and 1 M KOH solution, respectively, with a sweep rate of 50 mV s^{-1} from the range of -0.05 to 0.05 V. The electrochemical stability of the catalyst at 10 mA was measured by the chronopotentiometry. All the hydrogen evolution reaction (HER) polarization curves were showed by linear sweep voltammetry (LSV) at 5 mV s^{-1}, and the selection of electrolytes are the same as CV measurements. Electrochemical impedance spectroscopy (EIS) was performed at the overpotential of 10 mA cm^{-2} with frequency from 0.1~100 KHz. The electrochemically active surface area (ECSA) of samples was estimated by CV measurements. The current density was measured from 20 mV

to 100 mV with 20 mV S^{-1} increasing, in the case of the voltage range from 0.1 V to 0.2 V (E vs RHE). The electrochemical double-layer capacitance (C_{dl}) is from linear fitting, and the slope is the C_{dl} value.

Figures and Table

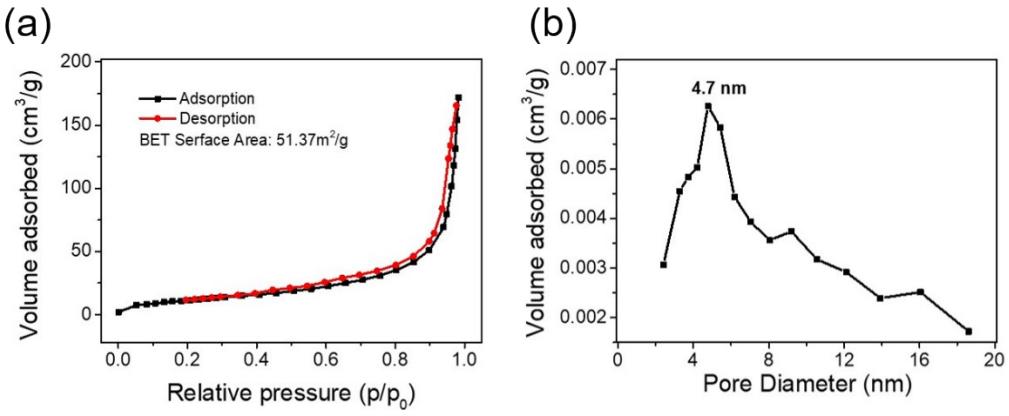

Figure S1. (a) BET adsorbates and adsorbents curves of Rh_2Ir NDs with adsorptive of N_2. (b) BET pore diameter curves of Rh_2Ir NDs.

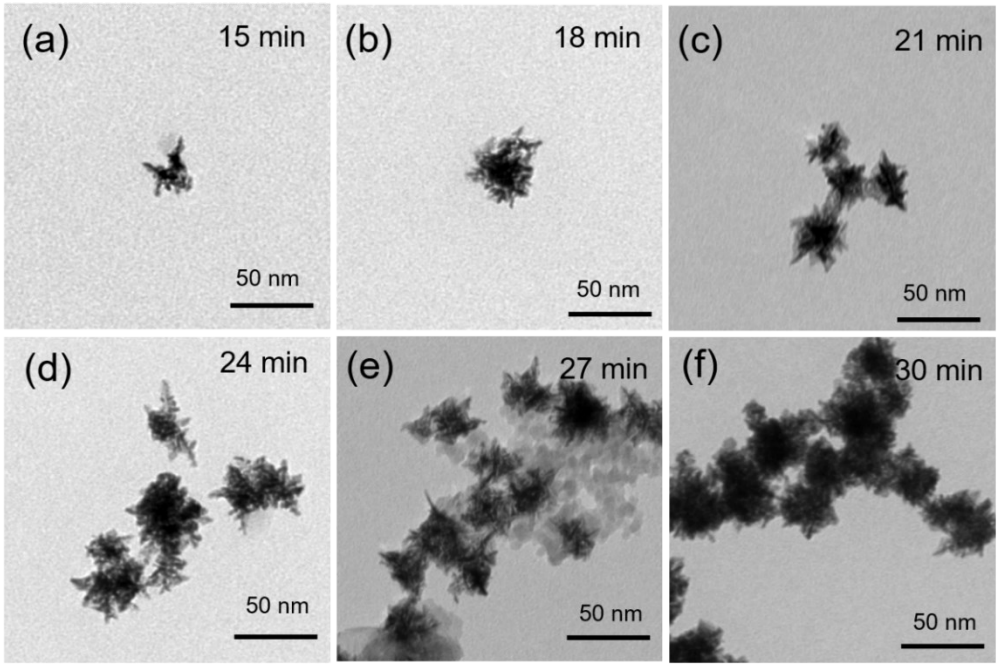

Figure S2. TEM images of Rh_2Ir NDs growth process for 15, 18, 21, 24, 27 and 30 minutes.

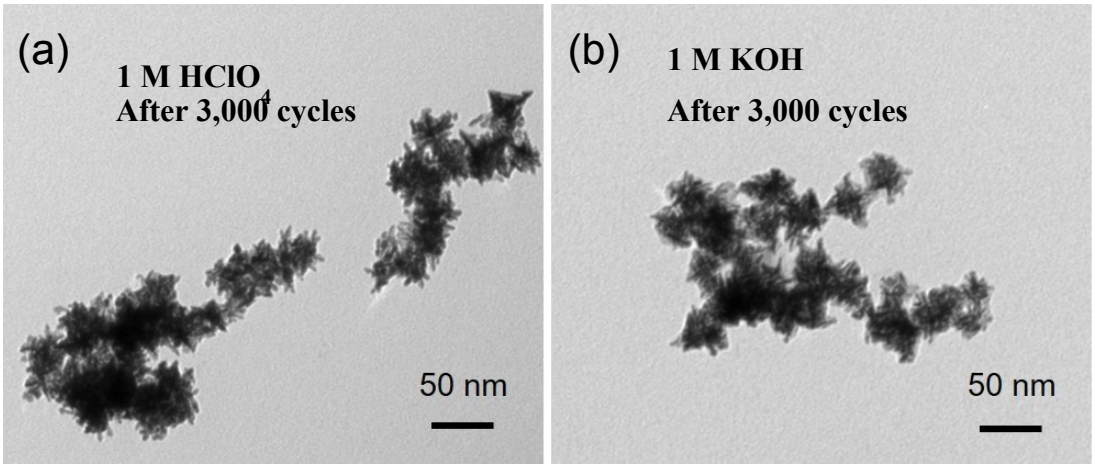

Figure S3. TEM image of Rh_2Ir NDs after 3,000 cycles in (a) acid and (b) alkaline conditions, respectively.

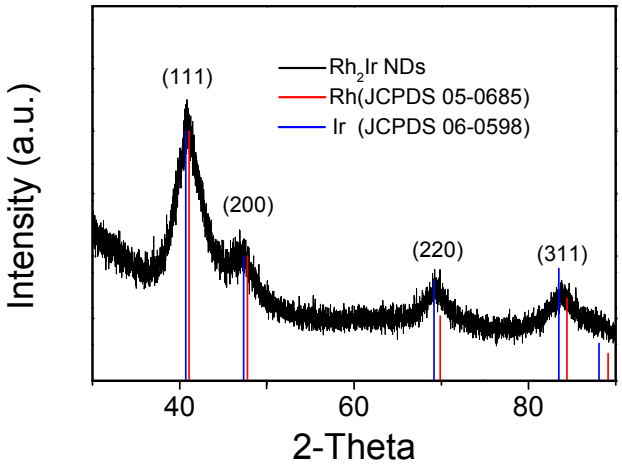

Figure S4. XRD spectrum of Rh_2Ir NDs after 3,000 cycles in alkaline condition.

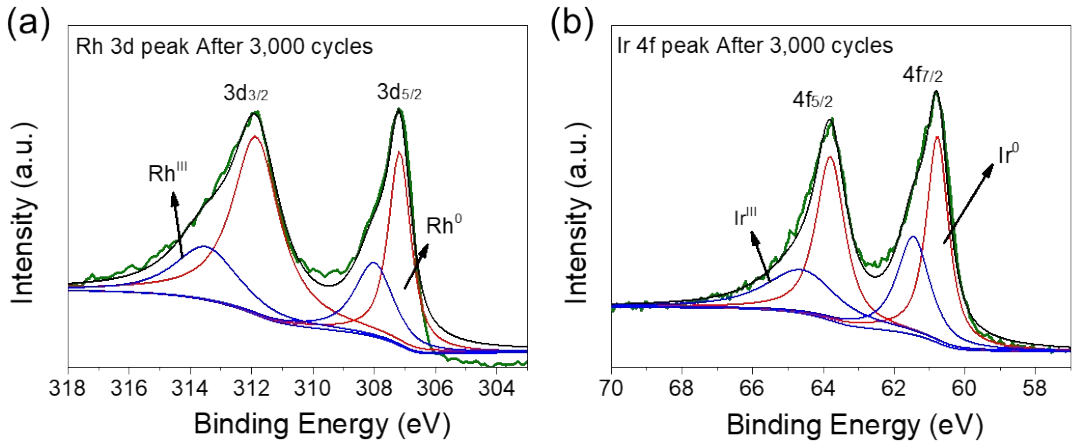

Figure S5. XPS spectra of Rh 3d in recovered Rh_2Ir NDs; (b) XPS spectrum of Ir 4f in recovered Rh_2Ir NDs.

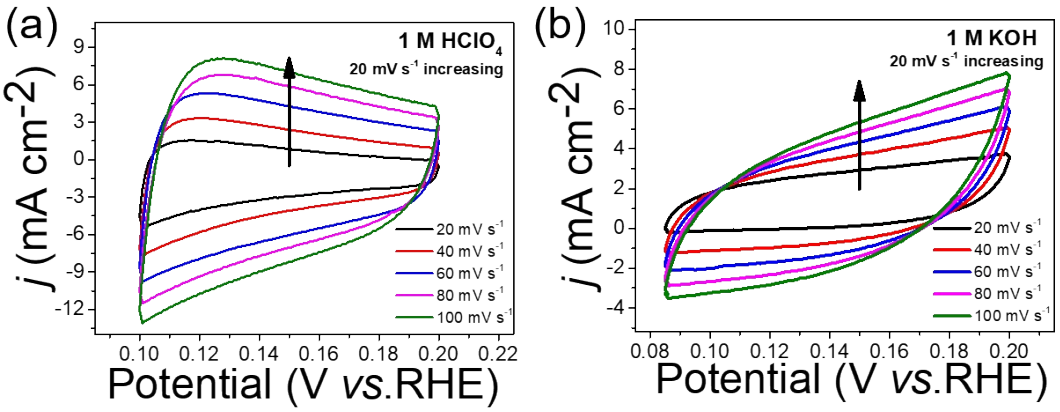

Figure S6. (a) ECSA of Rh_2Ir NDs in acid medium; (b) ECSA of Rh_2Ir NDs in alkaline medium.

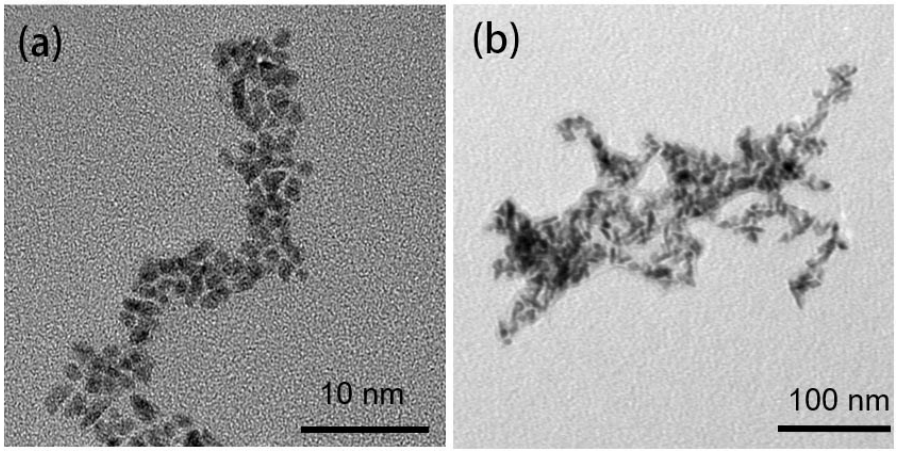

Figure S7. TEM images of (a) RhIr and (b) pure Rh samples.

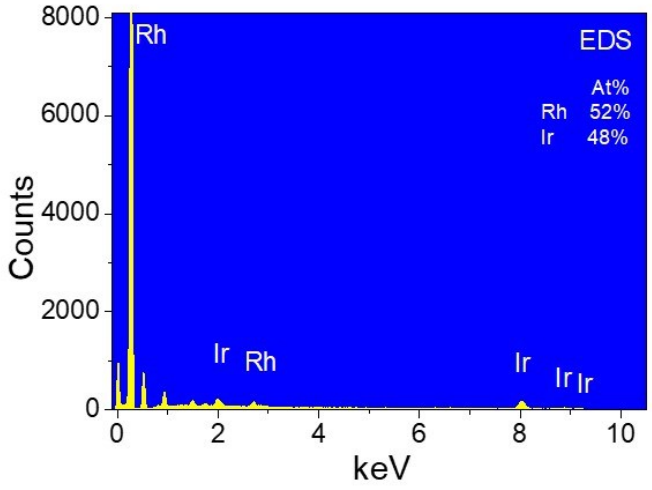

Figure S8. EDS spectrum of RhIr sample.

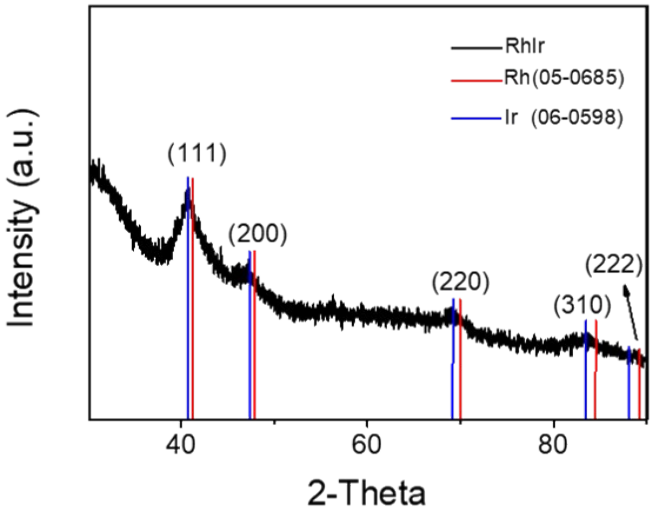

Figure S9. XRD pattern of RhIr sample.

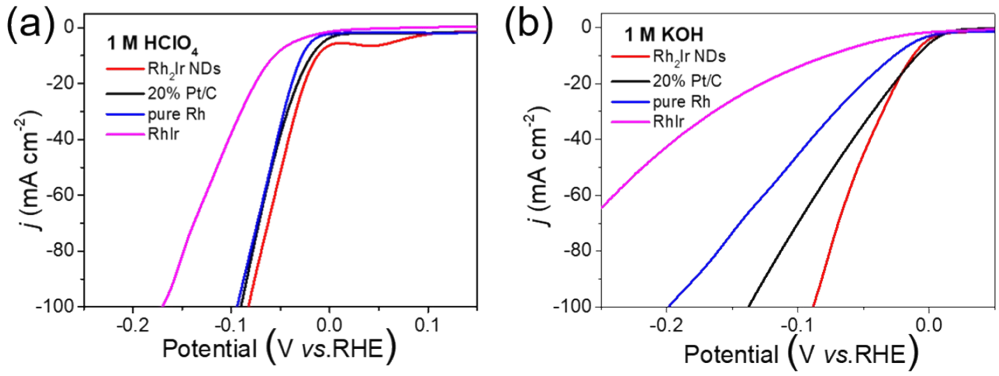

Figure S10. (a) LSV curves of comparation samples in acid medium; (b) LSV curves of comparation samples alkaline medium

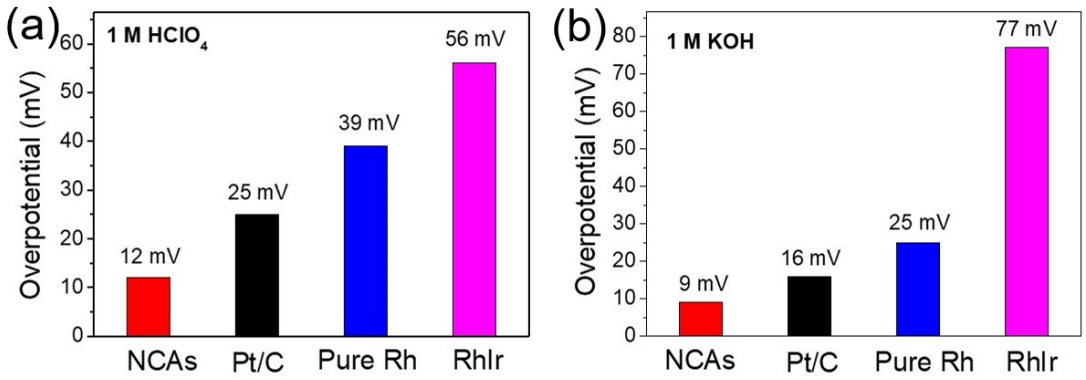

Figure S11. (a) Overpotential of comparation samples in acid medium; (b) Overpotential of comparation samples alkaline medium.

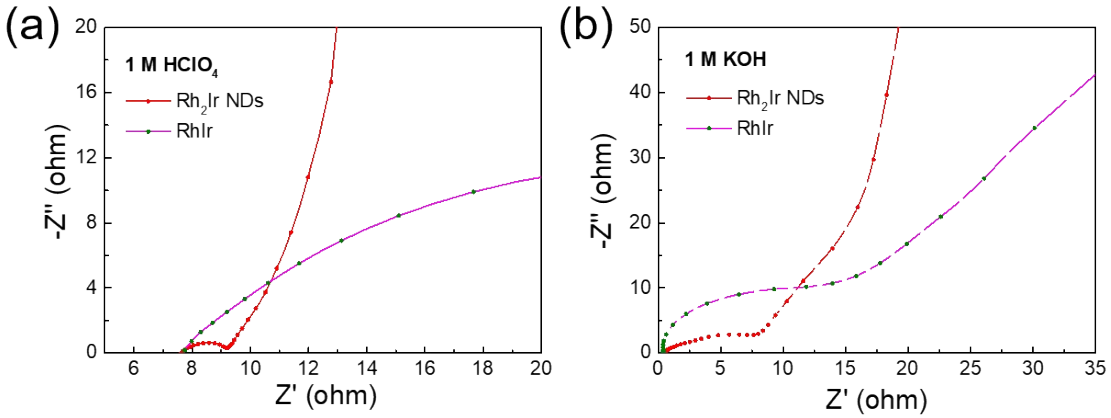

Figure S12. EIS curves of Rh_2Ir NDs and RhIr in (a) acid and (b) alkaline media.

Table S1. Comparison of relevant metal electrocatalysts for the HER reported before. (Alkaline)

Catalysis	Electrolyte	Overpotential (mV)	Tafel Slope (mV dec^{-1})	Reference
Rh_2Ir NDs	1 M KOH	9	25.8	This Work
IrRh sheet	1 M KOH	35	48.4	[1]
Co-Pt-NC	1 M KOH	50	48	[2]
RhO_2 particle	1 M KOH	14	30	[3]
PtRh	0.5 M KOH + 0.5 M EG	20	63.3	[4]
Rh-$MoSe_2$	1 M KOH	31	40	[5]
Rh@NG	0.1 M KOH	45	30	[6]
Rh-Si	1 M KOH	130	24	[7]
Ir_4Ru	1 M NaOH	32	32.9	[8]
NG@IrCo/NG	1 M KOH	49	30	[9]
Ru/CoO	1 M KOH	55	70	[10]
SA-Ru/Ru NPs/PC	1 M KOH	33	29	[11]
Pd–Ru@NG	1 M KOH	28	42	[12]
Mo_2C@NeC	1 M KOH	210	69	[13]

Table S2. Comparison of relevant metal electrocatalysts for the HER reported before. (Acid)

Catalysis	Electrolyte	Overpotential (mV)	Tafel Slope (mV dec^{-1})	Reference
Rh_2Ir NDs	1 M $HClO_4$	12	17.3	This Work
Hollow Pt NPs	0.5 M H_2SO_4	37	31	[14]
Co-Pt-NC	0.5 M H_2SO_4	27	31	[2]
Rh@NG	0.5 M H_2SO_4	29	30	[6]
PtCoIr NWs	0.1 M $HClO_4$	14	～	[15]
IrCo NFs	0.1 M $HClO_4$	24	35.3	[16]
IrCo/C	0.1 M $HClO_4$	24	26.6	[17]
Pd–Ru@NG	1 M H_2SO_4	39	60	[12]

References

1. C. Li, Y. Xu, S. Liu, S. Yin, H. Yu, Z. Wang, X. Li, L. Wang and H. Wang, *Acs Sustain Chem Eng*, 2019, **7**, 15747-15754.

2. L. Zhang, Y. Jia, H. Liu, L. Zhuang, X. Yan, C. Lang, X. Wang, D. Yang, K. Huang, S. Feng and X. Yao, *Angew Chem Int Ed Engl*, 2019, **58**, 9404-9408.

3. Z. Li, Y. Feng, Y. L. Liang, C. Q. Cheng, C. K. Dong, H. Liu and X. W. Du, *Adv Mater*, 2020, **32**, e1908521.

4. Y. X. Xie, S. Y. Cen, Y. T. Ma, H. Y. Chen, A. J. Wang and J. J. Feng, *J Colloid Interface Sci*, 2020, **579**, 250-257.

5. S. Liu, M. Li, C. Wang, P. Jiang, L. Hu and Q. Chen, *Acs Sustain Chem Eng*, 2018, **6**, 9137-9144.

6. J. Guan, X. Wen, Q. Zhang and Z. Duan, *Carbon*, 2020, **164**, 121-128.

7. L. Zhu, H. Lin, Y. Li, F. Liao, Y. Lifshitz, M. Sheng, S. T. Lee and M. Shao, *Nat Commun*, 2016, **7**, 12272.

8. Y. B. Cho, A. Yu, C. Lee, M. H. Kim and Y. Lee, *ACS Appl Mater Interfaces*, 2018, **10**, 541-549.

9. Z. Si, Z. Lv, L. Lu, M. Liu, Y. Chen, H. Jin, X. Tian, K. Dai, J. Liu and W. Song, *Chemcatchem*, 2019, **11**, 5457-5465.

10. J.-X. Guo, D.-Y. Yan, K.-W. Qiu, C. Mu, D. Jiao, J. Mao, H. Wang and T. Ling, *Journal of Energy Chemistry*, 2019, **37**, 143-147.

11. Q. Hu, G. Li, X. Huang, Z. Wang, H. Yang, Q. Zhang, J. Liu and C. He, *J Mater Chem A*, 2019, **7**, 19531-19538.

12. B. K. Barman, B. Sarkar and K. K. Nanda, *Chem Commun (Camb)*, 2019, **55**, 13928-13931.

13. G. Zhou, Q. Yang, X. Guo, Y. Chen, Q. Yang, L. Xu, D. Sun and Y. Tang, *Int J Hydrogen Energ*, 2018, **43**, 9326-9333.

14. Y. Wang, S. Ma, Q. Li, Y. Zhang, X. Wang and X. Han, *Acs Sustain Chem Eng*, 2016, **4**, 3773-3779.

15. Y. Sun, B. Huang, Y. Li, Y. Xing, M. Luo, N. Li, Z. Xia, Y. Qin, D. Su, L. Wang and S. Guo, *Chemistry of Materials*, 2019, **31**, 8136-8144.

16. L. Fu, X. Zeng, G. Cheng and W. Luo, *ACS Appl Mater Interfaces*, 2018, **10**, 24993-24998.

17. J. Feng, F. Lv, W. Zhang, P. Li, K. Wang, C. Yang, B. Wang, Y. Yang, J. Zhou, F. Lin, G. C. Wang and S. Guo, *Adv Mater*, 2017, **29**.